Size Exclusion Chromatography with Multiple Detectors: Solution Properties of Linear Chains of Varying Flexibility in Tetrahydrofuran

CHRISTIAN JACKSON,[1,*] YUAN-JU CHEN,[2] and JIMMY W. MAYS[2]

[1]Central Research and Development, E. I. duPont de Nemours and Company, Experimental Station, Wilmington, Delaware 19880-0228, and [2]Department of Chemistry, University of Alabama at Birmingham, Birmingham, Alabama 35294-1240

SYNOPSIS

Narrow molecular weight distribution polyisoprenes (PI), polybutadienes (PBD), poly(isobutylenes) (PIB), poly(methylmethacrylates) (PMMA), polystyrenes (PS), and poly(octadecyl methacrylates) (PODMA) have been studied by size exclusion chromatography (SEC) in tetrahydrofuran (THF) with light scattering and viscometric detectors. The molecular weight (M) dependence of the intrinsic viscosity, $[\eta]$, and radius of gyration, R_g, is reported for THF solutions of these polymers, in many instances for the first time. The availability of these data for a series of chains of varying flexibility allows a test of the universal calibration principle in SEC. Furthermore, an apparent dependence of the hydrodynamic parameter in good solvents, Φ, on chain stiffness is observed. All chains appear to exhibit hydrodynamic draining in THF. © 1996 John Wiley & Sons, Inc.

INTRODUCTION

The introduction and development of light-scattering and viscometry equipment suitable for use as molecular weight/size-sensitive detectors for size exclusion chromatography (SEC) has been one of the most significant developments in polymer characterization techniques over the past decade or so. Both low-angle (LALS)[1] and multiangle light-scattering (MALS)[2] units adaptable for use as SEC detectors are commercially available. The use of these devices in combination with a concentration sensitive detector (usually a differential refractometer or ultraviolet spectrometer) allows molecular weights and polydispersities to be measured directly without resorting to an SEC calibration curve. This is significant because conventional SEC requires calibration with standards of the same type as the polymer being analyzed if meaningful molecular weight data are to be obtained. This is a particular concern when analyzing branched polymers or copolymers by SEC. In addition to molecular weight information, a MALS detector can also provide the radius of gyration (R_g) of the particle, provided the polymer is not too small.[3] A knowledge of R_g can be very useful in determining the presence and extent of long-chain branching in polymers.

The most successful viscometer design for use in SEC has been the differential viscometer (DV) of Haney.[4] The effects of pulsing from the pump are minimized by measuring the difference in pressure between matched capillaries containing pure solvent and the dilute polymer solution. The use of SEC/DV allows molecular weights to be calculated using the universal calibration principle.[5] This principle invokes the idea that SEC separations are based on hydrodynamic volume (product of molecular weight, M, and intrinsic viscosity $[\eta]$). Thus, a plot of log $([\eta]M)$ vs. elution (V_e) is expected to be independent of the type and architecture of the polymer being analyzed. Commercially available polystyrene (or other) molecular weight standards are injected into the system, $[\eta]$ is measured, and the universal calibration is generated. This then allows M to be com-

* To whom correspondence should be addressed at DuPont Central Research and Development, P.O. Box 80228, Wilmington, DE 19880-0228.

Journal of Applied Polymer Science, Vol. 61, 865-874 (1996)
© 1996 John Wiley & Sons, Inc. CCC 0021-8995/96/050865-10

puted from a measurement of $[\eta]$ for any "unknown" material.

In this article we report the results of SEC/MALS/DV experiments in tetrahydrofuran (THF) for six different series of narrow molecular weight distribution polymers: polybutadiene (PBD), polyisoprene (PI), poly(isobutylene) (PIB), polymethyl methacrylate) (PMMA), polystyrene (PS), and poly (octadecylmethacrylate) (PODMA). The data obtained lead to power relationships between R_g and M and $[\eta]$ and M. In some instances, the power law expressions in THF are reported for the first time for these polymers; This is significant because THF is the solvent most commonly used in SEC of synthetic polymers. In instances where power law relations are already available in THF, the data reported herein are generally in good accord with literature data. In addition, the data generated for this series of structurally diverse, linear polymers allow the influence of chain flexibility on the universal calibration to be evaluated. Chain flexibility can be defined in terms of Flory's characteristic ratio, C_∞.[6]

$$C_\infty = \lim_{N\to\infty} \frac{\langle r^2\rangle_o}{N\ell^2} \quad (1)$$

where $\langle r^2\rangle_o$ is the unperturbed (theta condition) mean-square end-to-end distance of a polymer having N main chain bonds of average length ℓ. The polymers studied exhibit characteristic ratios ranging from about 5 to about 20.[7] The larger the value of C_∞, the less flexible is the polymer chain. Furthermore, the combined measurements of M, R_g, and $[\eta]$ for these samples allow the influence of chain flexibility on the Flory hydrodynamic parameter Φ, defined as

$$\Phi = ([\eta]M)/(6^{3/2}R_g^3) \quad (2)$$

to be evaluated in the same good solvent. These data, in turn, allow a test of certain theories pertaining to hydrodynamic properties of polymers in solution.

EXPERIMENTAL

Materials

The polymers studied all had narrow molecular weight distributions generally $M_w/M_n \leq 1.05$). Most of the PS, PMMA, PBD, and PI samples were obtained from Polymer Laboratories (Amherst, MA). Some additional PS specimens were purchased from American Polymer Standards (Mentor, OH), and additional PBD, PI, and PMMA samples were synthesized by anionic polymerization. Low polydispersity PIB standards were obtained from American Polymer Standards. Some additional PIBs, synthesized by living cationic polymerization, were obtained from Professor Robson Storey of the University of Southern Mississippi. PODMA specimens were produced by polymerization of octadecyl methacrylate (Polysciences, Warrington, PA) having azobisisobutyronitrile in benzene under vacuum conditions, followed by solvent/nonsolvent fractionation. Polymer microstructure in these materials is considered, based upon their mode of preparation, to be independent of molecular weight. The polymer structures and their characteristic ratios are given in Table I. The solvent used was HPLC grade THF from E. M. Science (Gibbstown, NJ).

Instrumentation and Methods

The chromatograph was a Waters 150C ALC/GPC (Waters Associates, Milford, MA). Two SEC columns (300 × 7.5 mm i.d.), packed with 20 μm mixed pore size (Mixed-A) PLgel particles (Polymer Laboratories), were used in series. Polymer solutions were prepared with concentrations from 0.25 mg/mL to 2.0 mg/mL. The higher concentrations were used for lower molecular weight samples; 100 μL of polymer solution was injected onto the columns for each measurement. The sample concentrations were measured using the differential refractometer contained in the Waters 150C unit. The refractometer was calibrated with a series of solutions of different concentrations and known refractive indices. This avoids any problems with the peak mass not corresponding to the injection mass and, thus, increases the measurement precision.

The light-scattering detector was a DAWN Model F MALS photometer (Wyatt Technology, Santa Barbara, CA) fitted with a Model 2014 10 mW argon ion laser tuned to 488 nm emission (Uniphase, San Jose, CA). The scattering cell was made from K5 glass with a refractive index of 1.52844 (at 488 nm). The argon ion laser was used, rather than the (2 mW) helium neon laser that is usually installed in the DAWN unit, because the greater power and shorter wave length results in increased scattering intensity and also improves the sensitivity of the radius of gyration measurements by increasing the magnitude of the scattering vector. A low refractive index glass cell was used in order to minimize the refractive index change at the cell/solvent interface and reduce internal scattering in the detection cell. The detector measures the scattered light intensity

Table I Structures and Characteristic Ratios of Polymers Studied

Polymer	Structure	C_∞	Ref.
Polyisoprene	$-(CH=CHCH_2CH_2)_n-$ with CH_3	4.7	9
Polybutadiene	$-(CH=CHCH_2CH_2)_n-$	4.9	9
Polyisobutylene	$-(C(CH_3)_2-CH_2)_n-$	6.6	9
Poly(methyl methacrylate)	$-(C(CH_3)(COOCH_3)-CH_2)_n-$	6.9	9
Polystyrene	$-(CH(C_6H_5)-CH_2)_n-$	10.0	9
Poly(octadecyl methacrylate)	$-(C(CH_3)(COO(CH_2)_{17}CH_3)-CH_2)_n-$	20.4	10

simultaneously at 15 different angles in the plane perpendicular to the plane of polarization of the incident beam. The photodetectors cover a range typically from 20 to 150° with respect to the incident beam direction. The actual observed angles depend on the refractive index of the solution due to refraction at the cell/solvent interface. The cell geometry is such that the solvent flows through a circular bore in the cell that runs coaxially with the incident beam.

The weight-average molecular weight, M_w, is derived from SEC/MALS using the equation

$$M_w = \left(\frac{K_c}{R(\theta, o)}\right)_{c \to o}^{-1} \tag{3}$$

where K is the usual light scattering optical constant, c is concentration, and $R(\theta, o)$ is the excess Raleigh ratio extrapolated to zero angle. The very low concentrations used in SEC allow the direct use of eq. (3), which neglects the contribution of the second virial coefficient A_2. The z-average radius of gyration, $R_{g,z}$, is evaluated from the particle scattering function, $P(\theta)$, by the equation

$$\frac{1}{P(\theta)} + 1 + q^2 \frac{R_{g,z}^2}{3} \tag{4}$$

where q is the scattering vector equal to $(4\pi)/\lambda \sin(\theta/2)$. The refractive index increment dn/dc, in THF at 488 nm and 30°C were measured using a Wood refractometer and are listed in Table II. The molecular weights and radii reported correspond to peak values, and they are, thus, designated by M and R_g.

The continuous viscometer was a Viscotek Model 110 four-capillary bridge viscometer (Viscotek Corporation, Houston, TX). Measurement of the specific viscosity (η_{sp}) requires that both the solution

Table II Refractive Index Increments for the Polymers Studied in THF at 488 nm and 30°C

Polymer	dn/dc (mL/g)
PI	0.129
PBD	0.133
PIB	0.125
PMMA	0.089
PS	0.199
PODMA	0.075

Table III Results for Polyisoprene in THF

Sample	M (g/mol)	R_G (nm)	$[\eta]$ (dL/g)
PI-1	1,490	—	0.044
PI-2	2,900	—	0.067
PI-3	7,940	—	0.123
PI-4	11,100	—	0.153
PI-5	28,600	—	0.290
PI-6	67,600	—	0.535
PI-7	96,200	13.1	0.681
PI-8	326,600	26.8	1.680
PI-9	625,100	41.0	2.713
PI-10	1,479,000	71.7	5.176

and the solvent viscosity be measured at the same flow rate. This is achieved by measuring the solvent viscosity using a reference capillary. When solvent is flowing through the viscometer there is zero differential pressure; when the polymer is eluting, a differential pressure is measured. The specific viscosity is calculated from the ratio of the differential pressure to the pressure drop across the bridge. The intrinsic viscosity is taken as the ratio η_{sp}/c, due to the very small concentrations used in the SEC experiments.

The three detectors, refractometer, viscometer, and light-scattering photometer, can be arranged in various configurations after the SEC columns. After experimentation with various combinations, it was determined that an arrangement of columns to photometer to viscometer to refractometer was most advantageous and resulted in the sharpest peaks. Interdetector volumes were determined using the difference in peak onsets for narrow molecular weight polystyrene excluded from the columns.[8]

RESULTS AND DISCUSSION

For each sample the values of the molecular weight, radius of gyration, and intrinsic viscosity at the maximum of the concentration detector chromatogram peak were used, rather than any average values, in order to avoid any errors due to differences in polydispersity between the samples. The data are shown in Tables III–VIII. R_g values smaller than about 12 nm are not reported due to the lack of precision in the measurement for molecules below this size. In Table VIII, values of these parameters for unfractionated PODMA samples are also given.

The Mark–Houwink plots of $\log[\eta]$ vs. $\log M$ for the six polymers are shown in Figures 1–6. For the

Table IV Results for Polybutadiene

Samples	M (g/mol)	R_G (nm)	$[\eta]$ (dL/g)
PB-1	850	—	0.035
PB-2	2,780	—	0.069
PB-3	8,280	—	0.194
PB-4	18,600	—	0.307
PB-5	20,900	—	0.331
PB-6	36,200	—	0.525
PB-7	69,800	12.5	0.844
PB-8	83,200	14.5	0.996
PB-9	93,400	14.4	1.064
PB-10	101,300	15.8	1.088
PB-11	124,700	17.6	1.257
PB-12	162,200	20.6	1.533
PB-13	231,200	25.4	2.005
PB-14	272,900	27.6	2.255
PB-15	414,000	36.0	2.958
PB-16	519,900	41.2	3.541
PB-17	708,000	49.3	4.650
PB-18	758,400	52.4	4.641
PB-19	1,060,000	64.9	6.014

polymers where the data cover only the high molecular weight range (PIB and PODMA), the results can be adequately described by a straight line. However, the data for polymers where sufficient data were available below 10,000 g/mol required a second order polynomial to fit the data as a smaller slope is observed in the low molecular weight regime (see Figs. 1, 4, and 5). The exception to this trend was the polybutadiene data where there is no apparent

Table V Results for Polyisobutylene

Sample	M (g/mol)	R_G (nm)	$[\eta]$ (dL/g)
PIB-1	38,100	—	0.260
PIB-2	87,900	—	0.459
PIB-3	122,600	14.0	0.548
PIB-4	229,300	20.6	0.824
PIB-5	433,200	30.3	1.327
PIB-6	616,900	36.5	1.619
PIB-7	712,800	40.4	1.771
PIB-8	890,000	45.1	2.108
PIB-501	26,100	—	0.212
PIB-502	20,600	—	0.172
PIB-504	50,800	—	0.309
PIB-505	94,600	12.0	0.479
PIB-508	55,300	—	0.339
PIB-509	37,600	—	0.274
PIB-510	72,100	—	0.405

Table VI Results or Poly(methyl methacrylate)

Sample	M (g/mol)	R_G (nm)	$[\eta]$ (dL/g)
PMMA-1	2,640	—	0.039
PMMA-2	6,540	—	0.061
PMMA-3	7,840	—	0.065
PMMA-4	13,940	—	0.088
PMMA-5	20,100	—	0.109
PMMA-6	35,200	—	0.161
PMMA-7	67,600	—	0.253
PMMA-8	132,300	12.8	0.391
PMMA-9	261,500	18.4	0.627
PMMA-10	485,100	26.5	0.977
PMMA-11	601,400	30.8	1.123
PMMA-12	1,498,000	54.1	2.225

change in the slope with decreasing molecular weight down to ($M \simeq 1000$).

This change in slope is due to the onset of the excluded volume effect. For low molecular weights, the polymer chain is not sufficiently long for excluded volume to affect the dimensions; only above a certain molecular weight does it become significant. Although such data are often fitted by two lines, the onset of the excluded volume effect is gradual, rather than a sharp transition, and polynomial fitting is used in this work. The change in slope is not seen for PBD probably because this is, along with PI, the most flexible chain and has a "streamlined" repeating unit of low molecular weight. Thus, excluded volume effects start at very low molecular weights. This behavior has previously been noted for PBD in the good solvent cyclohexane.[11] In the cases where the slope of the Mark–Houwink plots did change, its value always decreased and approached 0.5. This is the value predicted for the nonfree-draining polymer chain, indicating that even at molecular weights too low for excluded volume effects to occur, the polymer behaves hydrodynamically as a sphere.

In Figure 7, the M and $[\eta]$ data of Figures 1–6 are presented on one plot. This allows the observation that as the molecular weight of the repeating unit increases, the changes in slope occur at increasingly high molecular weights, as expected. All the lines are nearly parallel in the high molecular weight regime except for the data for PIB, which has a significantly lower slope and crosses the other lines. This suggests that THF may be a thermodynamically less good solvent for PIB, as compared to the other polymers (see discussion of power law exponents below). Specific interactions of PIB with the solvent can also not be ruled out.[12] Application of the universal calibration principle[5] successfully reduces all data of Figures 1–6 to a single line (Fig.

Table VII Results for Polystyrene in THF

Sample	M (g/mol)	R_G (nm)	$[\eta]$ (dL/g)
PS-1	600	—	0.029
PS-2	1,200	—	0.034
PS-3	4,000	—	0.048
PS-4	5,000	—	0.056
PS-5	10,400	—	0.092
PS-6	29,500	—	0.176
PS-7	70,300	11.1	0.321
PS-8	170,400	17.2	0.601
PS-9	338,400	23.9	0.991
PS-10	521,300	30.6	1.337
PS-11	804,700	40.1	1.858
PS-12	1,144,000	50.2	2.425
PS-13	2,061,000	74.1	3.864
PS-14	2,911,000	90.9	5.041
PS-15	3,956,000	102.2	7.580

Table VIII Results for Poly(octadecyl methacrylate)

Sample	M (g/mol)	R_G (nm)	$[\eta]$ (dL/g)
PODMA 0[a]	2,851,000	65.6	1.784
PODMA 1[a]	2,271,000	53.4	1.503
PODMA 2[a]	960,800	33.4	0.772
PODMA 0-1	4,622,000	88.4	2.657
PODMA 0-2	4,615,000	87.0	2.652
PODMA 0-3	4,805,000	88.5	2.752
PODMA 0-4	2,799,000	63.0	1.772
PODMA 0-5	3,272,000	69.3	2.009
PODMA 0-6	1,702,000	45.3	1.209
PODMA 1-0	4,674,000	100.4	2.567
PODMA 1-1	8,421,000	126.9	4.486
PODMA 1-2	6,596,000	109.8	3.556
PODMA 1-3	5,894,000	102.1	3.224
PODMA 1-4	4,452,000	83.2	2.587
PODMA 1-5	2,793,000	61.6	1.779
PODMA 1-6	1,721,000	44.0	1.228
PODMA 2-0	2,431,000	55.9	1.611
PODMA 2-1	4,787,000	89.1	2.645
PODMA 2-2	3,792,000	76.1	2.233
PODMA 2-3	3,227,000	67.8	1.953
PODMA 2-4	1,996,000	49.8	1.354
PODMA 2-5	1,226,000	36.5	0.933
PODMA 2-6	996,800	31.5	0.796
PODMA 2-7	726,600	25.7	0.638
PODMA 2-8	461,500	19.2	0.458

[a] Unfractional polymers.

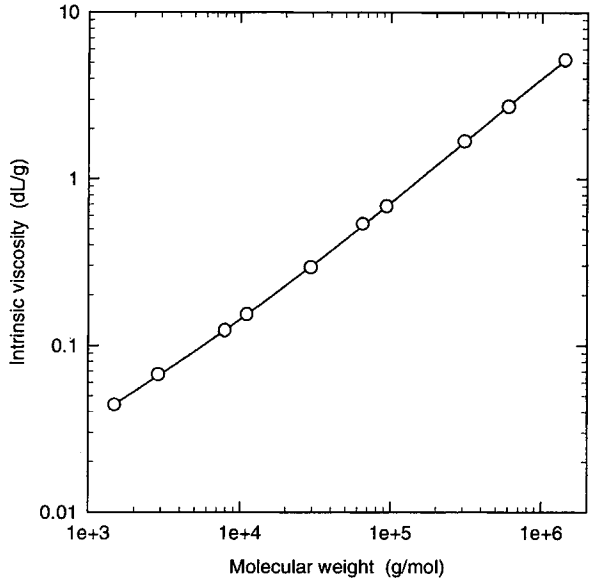

Figure 1 Mark–Houwink plot for polyisoprene in THF.

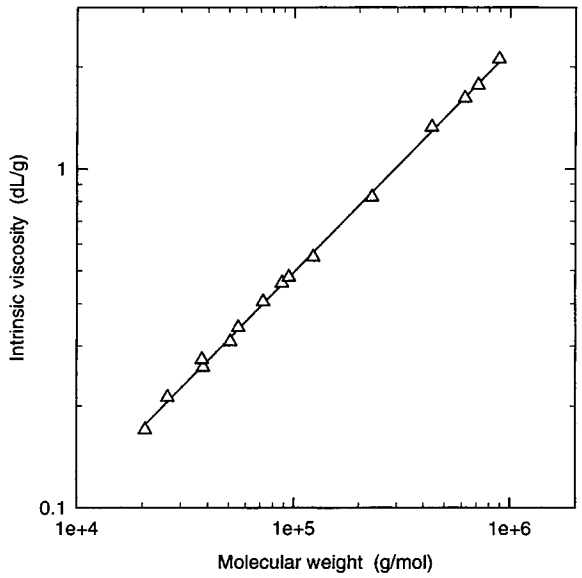

Figure 3 Mark–Houwink plot for poly(isobutylene) in THF.

8). Thus, the classical idea of universal calibration works effectively for the structurally diverse molecules of the present study.

The Mark–Houwink coefficients, taken from the linear portions of Figures 1–6, are presented in Table IX. The coefficients for PI are in good accord with those reported previously by Kraus and Stacy[13] ($K = 1.77 \times 10^{-4}$ and $a = 0.735$). For PBD, the findings for these parameters are almost identical to those reported by Xu et al.[14] ($K = 2.56 \times 10^{-4}$ and $a = 0.74$), but are appreciably different from parameters reported by Colby et al.[15] For PIB, we are not aware of any prior literature data for this polymer/solvent system. In the cases of PMMA and PS, the Mark–Houwink parameters of Table IX generate $[\eta]$ values that are only slightly smaller (by ca. 10%) than those generated using equations reported previously for these systems.[11,16] The only large discrepancy between the present and prior results for the Mark–Houwink coefficients is seen for PODMA. The expression reported by Xu and co-workers[10]

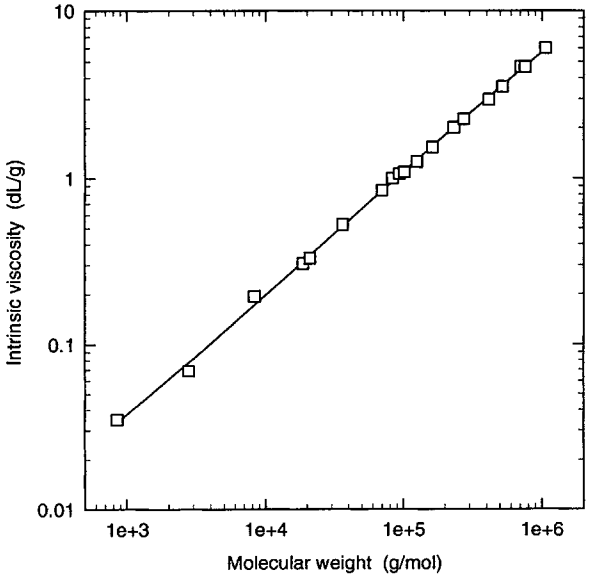

Figure 2 Mark–Houwink plot for polybutadiene in THF.

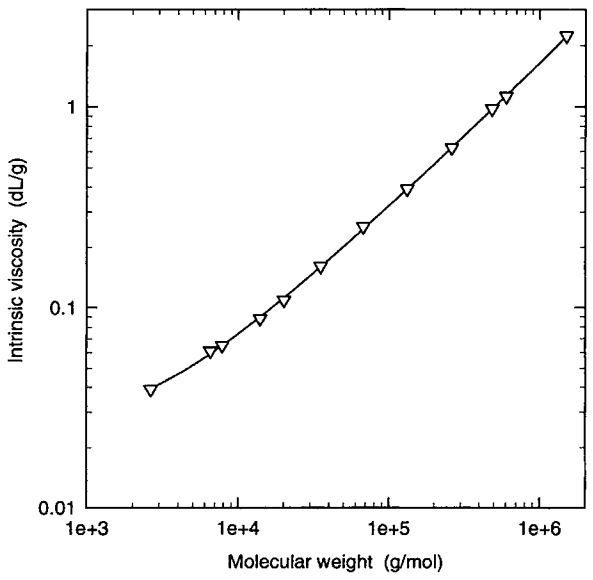

Figure 4 Mark–Houwink plot for poly(methyl methacrylate) in THF.

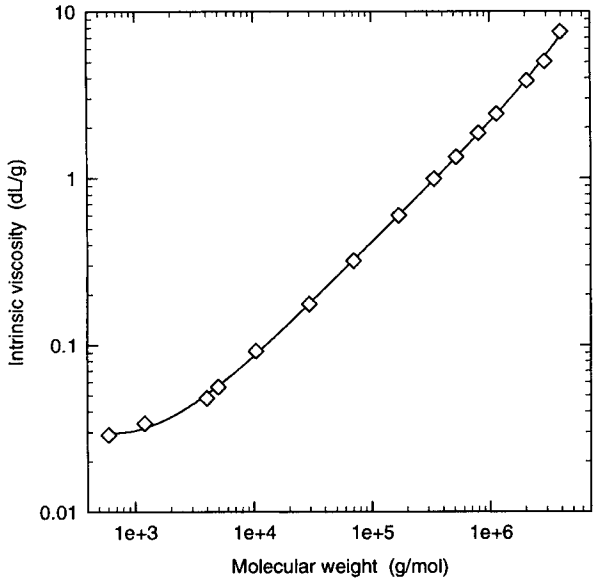

Figure 5 Mark–Houwink plot for polystyrene in THF.

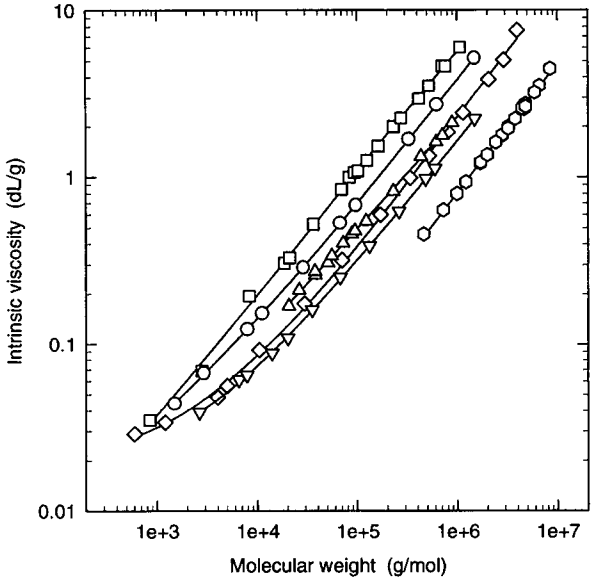

Figure 7 Mark–Houwink plots for all six polymers in THF. Symbols are the same as in Figures 1–6.

gives $K = 8.95 \times 10^{-5}$ and $a = 0.67$. However, the molecular weight range studied in the prior work is much lower. Because full excluded volume interactions are expected only at very high molecular weights for this polymer, this may well explain the much larger exponent measured in the present work. Also, it must be noted that polydispersity effects could play a role here. Although fractionated samples having polydispersity ratios of about 1.3 or less were used in both studies, only in the present study were effects of polydispersity on the measured parameters accounted for.

As a further example of the validity of $[\eta]$ and M values measured by the on-line configuration, we present the Burchard–Stockmayer–Fixman[17,18] plots of data for PI, PMMA, PS, and PODMA in Figure 9. From the intercepts of these plots we obtain the values of the Flory–Fox parameter K_θ for these

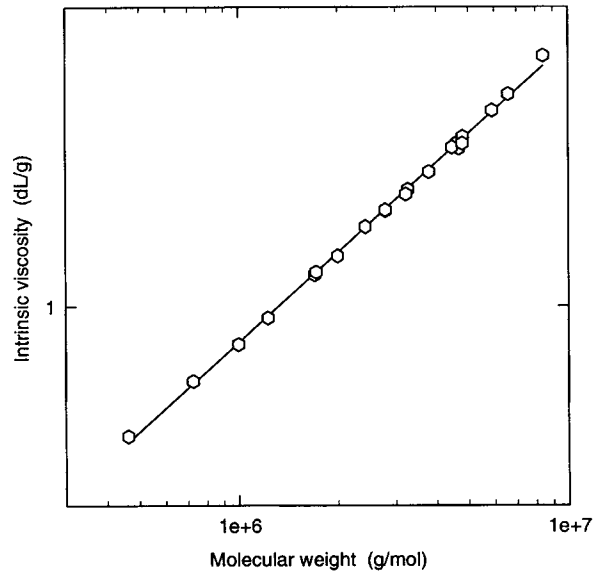

Figure 6 Mark–Houwink plot for poly(octadecyl methacrylate) in THF.

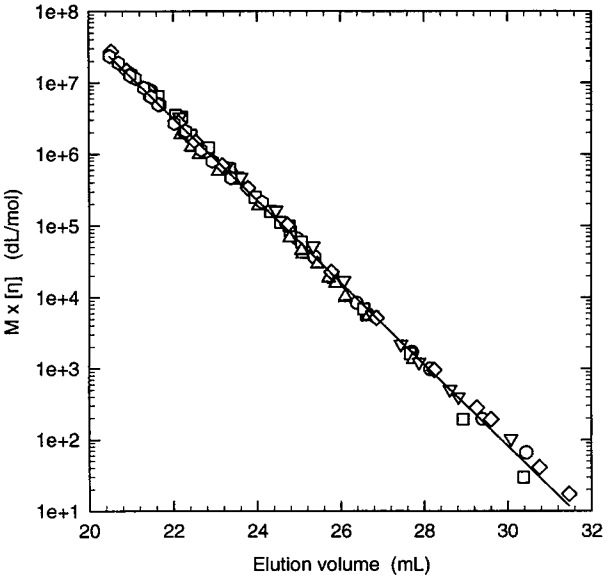

Figure 8 Universal calibration plot based on hydrodynamic volume ($[\eta] \times M$) for all six polymers in THF. Symbols are the same as Figures 1–6.

Table IX Mark–Houwink Coefficients in THF

Polymer	K (dL/g × 10^4)	a	r
PI	1.57	0.731	0.9999
PB	2.52	0.727	0.9996
PIB	2.66	0.654	0.9992
PMMA	0.897	0.710	0.9992
PS	0.863	0.736	0.9997
PODMA	0.160	0.783	0.9994

polymers. From K_θ, the unperturbed mean-square end-to-end distances $\langle r_2 \rangle_o$ can be evaluated from

$$K_\theta = \Phi_o(\langle r^2 \rangle_o / M)^{3/2} \quad (5)$$

where the Flory hydrodynamic parameter Φ_o is taken as approximately equal to 2.7×10^{21} mol^{-1}.[20] C_∞ may then be calculated using eq. (1). This approach leads to C_∞ values of 4.6, 7.0, 9.9, and 20 for PI, PMMA, PS, and PODMA, respectively. These values agree well with the literature values for C_∞ that are given in Table I.

One very interesting observation concerning Figure 9 is that the data for PODMA are linear over the entire range of molecular weight, whereas distinct downward curvature is observed for the other polymers at high molecular weights. Because the curvature is normally attributed to the breakdown of the two-parameter theory, upon which the Burchard–Stockmayer–Fixman procedure is based, for large excluded volumes,[20] this is an indication that extremely high molecular weights are necessary for large excluded volumes in the case of the PODMA/THF system.

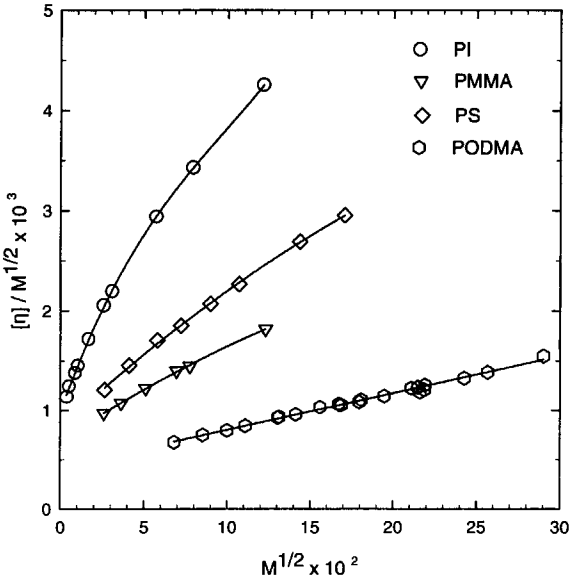

Figure 9 Burchard–Stockmayer–Fixman plot for polyisoprene, poly(methyl methacrylate), polystyrene, and poly(octadecyl methacrylate) in THF.

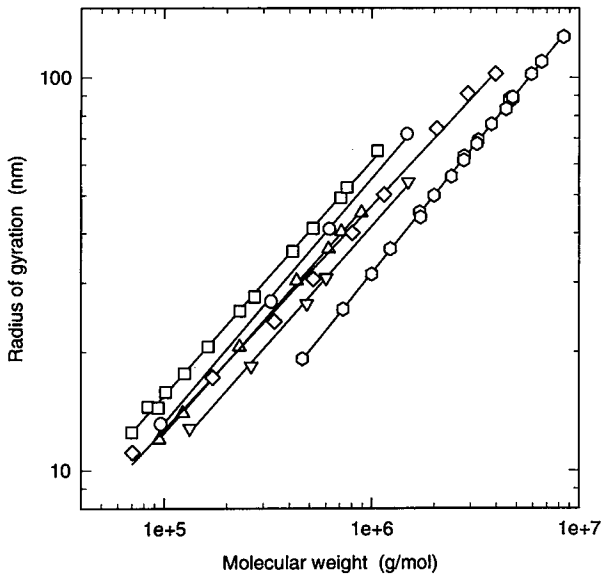

Figure 10 Radius of gyration against molecular weight for all six polymers in THF. Symbols are the same as in Figures 1–6.

Figure 10 shows a log–log plot of radius of gyration against molecular weight for the six polymers studied. All relationships appear to be linear over the entire range of molecular weight and can be described by the scaling relationship

$$R_g = K'M^\upsilon \quad (6)$$

The power law exponents, υ, and prefactors K', derived from the data of Figure 9, are presented in Table X. Extensive data on R_g in THF for the polymers of this work with the exception of PS, are lacking in the literature. Even for PS, the literature data on R_g from various groups are not in very good

Table X Radius of Gyration Scaling Coefficients

Polymer	K' (nm × 10^2)	υ	r
PI	1.22	0.609	0.9994
PB	1.60	0.597	0.9994
PIB	1.46	0.586	0.9971
PMMA	1.10	0.596	0.9992
PS	1.118	0.600	0.9988
PODMA	0.392	0.652	0.9993

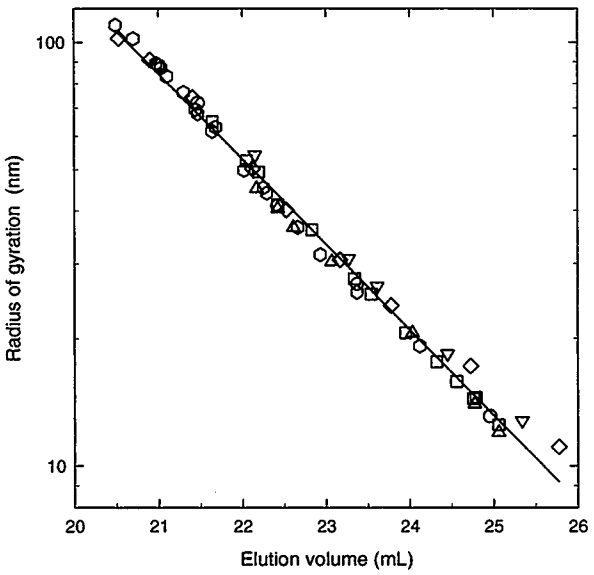

Figure 11 Calibration curve of log R_g plotted against SEC elution volume for the six polymers studied. Symbols are the same as in previous plots.

agreement, as pointed out in a recent review.[11] The exponent of 0.609 for PI in THF is a bit higher than the value of 0.6 that is expected in a thermodynamically good solvent, but the parameters reported for PI in Table X are almost identical to those reported recently for this polymer in cyclohexane,[11] based upon a consideration of all available literature data. Small microstructural variations in PI samples could be the reason for these slightly larger than expected values. The exponent for PIB is lower than for any of the other polymers suggesting, as noted above, that THF is not as good a solvent for this polymer as for the others. The exponent of 0.652 observed for PODMA is probably a reflection of the diminished conformational flexibility of this polymer, which has the highest C_∞ value of all polymers studied in this work. Even at the highest molecular weights studied this polymer does not achieve flexible chain behavior, and the data may be better described by the wormlike chain model.

In Figure 11, log R_g vs. elution volume is plotted for the various polymers. The greater scatter in Figure 11, as compared to Figure 8, suggests that hydrodynamic size ($[\eta]M$) more closely defines the SEC separation mechanism than does R_g, although it may be due to the poorer precision of the R_g measurement.

From the data of Tables III–VIII we can compute the ratio of the good solvent hydrodynamic parameter Φ [defined by eq. (2)] to its theta solvent value Φ_0. Because Yamakawa and his collaborators[19] have shown that the magnitude of Φ_0 is dependent to some extent on the nature of the polymer and solvent, we have used actual literature values of Φ_0 instead of assuming a constant value. For PI, PBD, and PIB we utilize $\Phi_0 = 2.5 \times 10^{21}$ mol^{-1}, the value calculated from the compilation of data in ref. 11. For PMMA and PS, we utilize the average values of 2.3×10^{21} and 2.6×10^{21} reported by Fujii et al.[19] for PMMA and PS, respectively, in two different theta solvents. For PODMA data extrapolated to the theta condition yield $\Phi = 1.3 \times 10^{21}$;[21] this value seems to be unrealistically small because the Φ values of the present work, determined in the good solvent THF, are actually larger. Thus, we utilize an estimate of $\Phi_0 \simeq 2.5 \times 10^{21}$ for this polymer. The Φ_0 values are not corrected for polydispersity, which is very small in the chains investigated.

The computed values of Φ/Φ_0 are plotted against the radius of gyration expansion factor α_s in Figure 12. For PI, PBD, PIB, and PS the necessary theta condition R_g values are taken from ref. 11. For PMMA, the R_g data of Fujii et al.[19] are employed. For PODMA we utilize the K_θ value of 3.71×10^{-4} dL/g reported by Xu and co-workers[10] to compute the intrinsic viscosity expansion factor α_η from:

$$\alpha_\eta = ([\eta]/[\eta]_\theta)^{1/3} \tag{7}$$

Renormalization group theory predicts an asymptotic Φ/Φ_0 value of 0.897 in the least-draining limit.[22] Smaller values of Φ/Φ_0 have been attributed

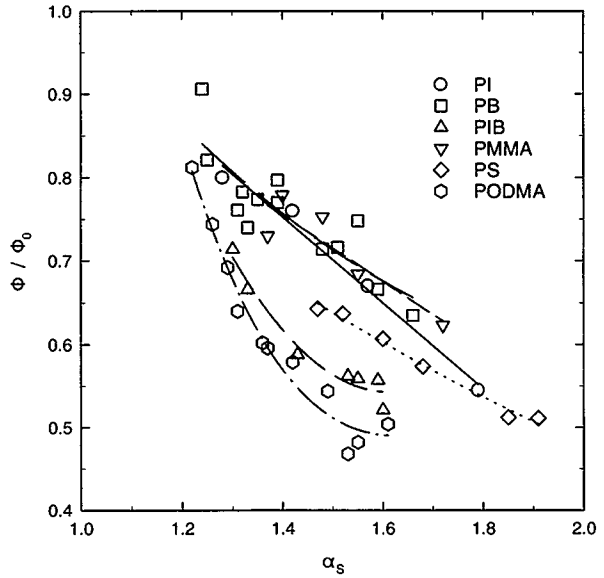

Figure 12 Normalized Flory viscosity function Φ/Φ_0 against the radius of gyration expansion factor α_s for the six polymers in THF.

to enhanced draining of solvent through the coil.[23] It is clear from Figure 11 that all the polymers studied in this work exhibit draining in THF. Close inspection of Figure 11 shows some indications of a dependence of extent of draining on the chain flexibility parameter C_∞. The most tightly coiled chains, PI and PBD consistently exhibit larger Φ/Φ_0 values at a given chain expansion than PODMA, the least flexible chain. The data for PIB are interesting, because this chain exhibits an extent of draining that is almost as great as that of PODMA, despite its high flexibility. Also, the Φ/Φ_0 values reported recently[24] for PIB in the good solvent cyclohexane are larger than the values measured in this work. High levels of draining, based on small Φ/Φ_0 values, have also been observed for poly(*tert*-butylstyrene) in the good solvent cyclohexane.[25] This chain has a characteristic ratio of 12–13,[25] and the high degree of draining for this polymer is consistent with the trend of higher C_∞-higher draining observed in this work. Clearly, more studies are desirable to shed further light on this situation.

Jimmy W. Mays and Yuan-Ju Chen thank the DuPont Company for financial support.

REFERENCES

1. The Chromatix KMX-6 unit is sold commercially by LDC Analytical, Riviera Beach, FL.
2. The DAWN-F multiangle unit is available from Wyatt Technology, Santa Barbara, CA.
3. M. B. Huglin (Ed.), *Light Scattering From Scattering Polymer Solutions,* Academic, London, 1972.
4. Available from Viscotek Corporation, Houston, TX.
5. H. Benoit, Z. Grubisic, P. Rempp, D. Decker, and J. G. Zilliox, *J. Chim. Phys.*, **63,** 1507 (1966).
6. P. J. Flory, *Statistical Mechanics of Chain Molecules,* Wiley-Interscience, New York, 1969.
7. Z. Xu, N. Hadjichristidis, J. W. Mays, and L. J. Fetters, *Adv. Polym. Sci.*, **120,** 1 (1995).
8. T. H. Mourey and S. M. Miller, *J. Liquid Chromatogr.*, **13,** 693 (1990).
9. J. Brandrup and E. H. Immergut, Eds., *Polymer Handbook,* 3rd Ed., Wiley- Interscience, New York, 1989.
10. Z. Xu, N. Hadjichristidis, and L. J. Fetters, *Macromolecules,* **17,** 2303 (1984).
11. L. J. Fetters, N. Hadjichristidis, J. S. Lindner, and J. W. Mays, *J. Phys. Chem. Ref. Data,* **23,** 619 (1994).
12. T. P. Lodge, *J. Phys. Chem.*, **97,** 1480 (1993).
13. G. Kraus and C. J. Stacy, *J. Polym. Sci., Part A-2,* **10,** 657 (1972).
14. Z. Xu, M. Song, N. Hadjichristidis, and L. J. Fetters, *Macromolecules,* **14,** 1591 (1981).
15. R. H. Colby, L. J. Fetters, and W. W. Graessley, *Macromolecules,* **20,** 2226 (1987).
16. Y.-J. Chen, J. Li, N. Hadjichristidis, and J. W. Mays, *Polym. Bull.*, **30,** 575 (1993).
17. W. Burchard, *Makromol. Chem.*, **50,** 20 (1960).
18. W. H. Stockmayer and M. Fixman, *J. Polym. Sci., Part C,* **1,** 137 (1963).
19. Y. Fujii, T. Konishi, T. Yoshizaki, and H. Yamakawa, *Macromolecules,* **24,** 5614 (1991).
20. H. Yamakawa, *Modern Theory of Polymer Solutions,* Harper and Row, New York, 1971.
21. M. Ricker and M. Schmidt, *Makromol. Chem.*, **192,** 679 (1991).
22. K. F. Freed, *Renormalization Group Theory of Macromolecules,* Wiley-Interscience, New York, 1987.
23. K. F. Freed, S.-Q. Wang, J. Roovers, and J. F. Douglas, *Macromolecules,* **21,** 2219 (1988).
24. L. J. Fetters, N. Hadjichristidis, J. S. Linder, J. W. Mays, and W. W. Wilson, *Macromolecules,* **24,** 3127 (1991).
25. A. George, W. W. Wilson, J. S. Lindner, and J. W. Mays, *Polymer,* **25,** 600 (1994).

Received February 14, 1995
Accepted May 28, 1995